Molecular and Cellular Pathobiology

Cancer Research

Natural Allelic Variations in Glutathione Peroxidase-1 Affect Its Subcellular Localization and Function

Soumen Bera[1], Frank Weinberg[1], Dede N. Ekoue[1], Kristine Ansenberger-Fricano[2], Mao Mao[1,2], Marcelo G. Bonini[1,2], and Alan M. Diamond[1]

Abstract

Glutathione peroxidase 1 (GPx-1) has been implicated in the etiology of several common diseases due to the association between specific allelic variations and cancer risk. The most common among these variations are the codon 198 polymorphism that results in either a leucine or proline and the number of alanine repeat codons in the coding sequence. The molecular and biologic consequences of these variations remain to be characterized. Toward achieving this goal, we have examined the cellular location of GPx-1 encoded by allelic variants by ectopically expressing these genes in MCF-7 human breast carcinoma cells that produce undetectable levels of GPx-1, thus achieving exclusive expression in the same cellular environment. A differential distribution between the cytoplasm and mitochondria was observed, with the allele expressing the leucine-198 polymorphism and 7 alanine repeats being more cytoplasmically located than the other alleles examined. To assess whether the distribution of GPx-1 between the cytoplasm and mitochondria had a biologic consequence, we engineered derivative GPx-1 proteins that were targeted to the mitochondria by the addition of a mitochondria targeting sequence and expressed these proteins in MCF-7 cells. These cells were examined for their response to oxidative stress, energy metabolism, and impact on cancer-associated signaling molecules. The results obtained indicated that both primary GPx-1 sequence and cellular location have a profound impact on cellular biology and offer feasible hypotheses about how expression of distinct GPx-1 alleles can affect cancer risk. *Cancer Res; 74(18); 5118–26. ©2014 AACR.*

Introduction

Glutathione peroxidase 1 (GPx-1) is the ubiquitously expressed and best characterized member of the GPx family of selenium-containing proteins that uses reducing equivalents from glutathione to detoxify peroxides (extensively reviewed in ref. 1). The translation of GPx-1 includes the recognition of an in-frame UGA triplet as the codon for selenocysteine in a process that requires a selenocysteine insertion sequence in the 3′-untranslated region of the GPx-1 mRNA, a selenocysteine tRNA, and a host of selenoprotein-specific translation factors (2–5).

Support for a role for GPx-1 in cancer etiology comes from genetic data indicating significant associations between allelic variations in the GPx-1 gene and cancer risk (6, 7). Two GPx-1 common genetic variations have been extensively studied; an SNP resulting in either a proline (pro) or leucine (leu) variation at codon 198 or a variable number of alanine (ala) codon repeats that result in 5, 6, or 7 alanines in the amino terminus of the protein (reviewed in ref. 7). These variations are functional and interactive, determining the levels of GPx-1 enzyme activity for a given concentration of available selenium (8, 9). The *leu* allele has been associated with increased risk of cancers of several types, whereas no clear pattern of association has emerged about the number of Ala repeats (7). Recent data demonstrating the interactions between the amino acid at position 198 and the number of alanines may indicate that both variations may need to be considered when conducting studies assessing the role of allelic variations in *GPx-1* as it relates to affecting health outcomes (9). These genetic variations in *GPx-1* are not uncommon, with the proline/leucine-resulting polymorphism exhibiting an approximately 2:1 allele frequency, although the occurrence of the leucine/leucine homozygote genotype is 10% or less (10, 11). GPx-1 alleles encoding 5, 6, or 7 alanine-repeat codons in the 5′-terminus of that gene are present at frequencies that are approximately in a 2:1:1 ratio, although individuals homozygous for GPx-1 alleles with either the 5 or 6 codon repeat are uncommon (11, 12). The consequences of these variations on GPx-1 function are not understood, although *in vitro* and human data indicate interactions with enzyme activity and selenium availability, and in one study, gender as well (1).

To study the impact of allelic variations in GPx-1, we have taken advantage of the observation that human MCF-7 breast

[1]Department of Pathology, University of Illinois at Chicago, Chicago, Illinois. [2]Department of Medicine, University of Illinois at Chicago, Chicago, Illinois.

S. Bera and F. Weinberg contributed equally to this article.

Current address for S. Bera: School of Life Sciences, B.S. Abdur Rahman University, Seethakathi Estate, Vandalur, Chennai, TN 600048, India.

Corresponding Author: Alan M. Diamond, University of Illinois at Chicago, 840 South Wood Street, Room 10 CSN, Chicago, IL 60612. Phone: 312-413-8747; Fax: 312-996-7586; E-mail: adiamond@uic.edu

doi: 10.1158/0008-5472.CAN-14-0660

©2014 American Association for Cancer Research.

Downloaded from http://aacrjournals.org/cancerres/article-pdf/74/18/5118/2708352/5118.pdf by guest on 15 February 2025

carcinoma cells have negligible GPx enzyme activity and undetectable GPx-1 levels. Previously, we used these cells to exclusively express different GPx-1 alleles by transfection with allelic-specific GPx-1 expression constructs (8, 9). In this article, we used the same approach to further investigate the molecular and biologic consequences of allelic variations in the GPx-1 gene to gain a better understanding of the role of GPx-1 in cancer etiology.

Materials and Methods

Cell culture

MCF-7 cells were maintained in modified Eagle's medium (Gibco) supplemented with 10% FBS at 37°C with 5% CO_2. These cells were originally obtained from the ATCC and were authenticated by Genetetica DNA Laboratories on July 19, 2013, by analyses of 15 autosomal short tandem repeat loci and the gender identity locus amelogenein. The selenium concentration of the serum used was determined to be 152 nmol/L by graphite furnace atomic absorption spectrometry conducted at the Texas A&M Veterinary Diagnostic Laboratory at College Station, Texas, resulting in a final concentration of selenium in media containing 10% serum to be 15.2 nmol/L. Transfectants were generated using the Lipofectamine 2000 transfection reagent (Invitrogen) following the manufacturer's protocol and selected with 500 μg/mL G418 (Sigma), expanded, and screened for GPx-1 activity and expression. Cell survival and proliferation were assayed using the FluoReporter Blue Fluorometric dsDNA Quantitation Kit (InVitrogen).

Generation of allele-specific GPx-1 gene constructs

Previously generated GPx-1 expression constructs encoding 5 or 7 alanine repeats at the NH_2 terminus and either a proline or leucine at codon 198 were used as templates to generate mitochondrially targeted variants by fusion of the open reading frames to the mitochondrial targeting sequence (MTS) from the SOD2 gene. A primer containing an 87 nucleotide DNA sequence that included the 72 nucleotide MTS from the *SOD2* gene, as well as 15 nucleotides of the 5′-end of the human GPx-1 gene, shown underlined (5′-ATGTTGAGCCGGGCAGTGTGC-GGCACCAGCAGGCAGCTGGCTCCGGTTTTGGGGTATCTG-GGCTCCAGGCAGATGTGTGCTGCTCGG-3′), was obtained from Integrated DNA Technologies annealed to the DNA from individual GPx-1 expression constructs and extended using the Klenow fragment. The resulting hybrid DNA was amplified using a *Hind*III-containing forward primer (5′-GCAG-CAAAGCTTGCAGCATGTTG-3′) and a *ClaI*-containing reverse primer (5′-ATAATCGATTGACACCCGGCA-3′). The resulting PCR product was digested with *Hin*dIII and *Cla*1 and directionally inserted into the pLNCX retroviral vector (13).

Subcellular fractionation

Subcellular fractionation was performed using the standard procedure of Magalhães and colleagues (14). Briefly, cells were harvested by trypsinization, suspended in ice-cold mitochondria isolation buffer (250 mmol/L Sucrose, 10 mmol/L Tris-Cl, pH 7.4, and 1 mmol/L EDTA), and homogenized in a dounce-homogenizer. Efficient lysis was confirmed by viewing images under a light microscope with more than 60% of the cells having been ruptured. The cell lysate was centrifuged at 700 × *g* for 10 minutes at 4°C and the resulting supernatant was again centrifuged at 14,000 × *g* for 10 minutes at 4°C to pellet mitochondria, which were suspended in the isolation buffer.

GPx activity assay

GPx enzyme activity was determined on whole cell lysates, as well as the mitochondrial and cytosolic fractions, using a coupled spectrophotometric assay that determines the GPx-dependent consumption of NADPH (15). Enzyme activity was expressed as nmole NADPH oxidized per minute per milligram of total protein. In the text, we refer to the cellular activity determined by this assay as "GPx" activity as it cannot be completely ruled out that no other member of the GPx family of proteins contributed to the measured activity. For all experiments, cells were plated in triplicate and transfectants were maintained in G418, which was removed from the culture media 2 days before plating the cells to reduce any impact of that antibiotic on selenoprotein synthesis (16, 17).

Reactive oxygen species quantification

Oxidation of the reduction-oxidation sensitive green fluorescent protein (roGFP) and mito-roGFP probes was measured by flow cytometry. Briefly, cells were infected with adenoviral vectors expressing roGFP and mito-roGFP sensors at 100 plaque-forming unit per cell and incubated for 6 hours, after which time the virus-containing media were replaced with complete RPMI 1640 media and incubated overnight. Cells were harvested and equal aliquots were transferred to tubes with media, media with 1 mmol/L dithiothreitol, or media with 1 mmol/L *t*-butylhydroperoxide (*t*-BOOH). After incubation for 10 minutes at room temperature, the ratio of fluorescence emission at 535 nm and excitations at 405 and 488 nm was measured in 5,000 cells per sets using a Dako Cytomation CyAn ADP analyzer. The roGFP ratio was obtained by dividing the emission values obtained at 488 nm/535 nm by that obtained by 405 excitation/535-nm emissions. The oxidation state of the cells was calculated as the difference in the ratio observed with untreated values and completely reduced values divided by the difference in the ratio observed with dithiothreitol and t-BOOH. Values are represented as the percentage of oxidation of the probe with 100% being fully reduced and 1% being fully oxidized (18).

Confocal microscopy

Intracellular localization of GPx-1 was verified by confocal microscopy. Briefly, cells were plated on a 1.5-mm thick glass bottom culture dish (Mat Tek Corp) and incubated overnight, probed with 200 nmol/L Mitotracker red for labeling mitochondria, and then fixed with 4% paraformaldehyde at 37°C for 30 minutes. After fixation, cells were permeabilized and blocked with 3% BSA solution to minimize nonspecific binding of the primary antibody. Cells were incubated with a solution containing GPx-1 primary antibody (Aviva) for 45 minutes at room temperature followed by incubation with AlexaFluor-conjugated secondary antibody for 45 minutes at room temperature. Nuclear staining was achieved with 300 nmol/L DAPI, and cells were imaged using a Zeiss LSM510UV microscope.

Downloaded from http://aacrjournals.org/cancerres/article-pdf/74/18/5118/2708352/5118.pdf by guest on 15 February 2025

Seahorse Extracellular Flux assay

Cells were plated and grown on Seahorse Bioscience custom plates in Minimum Essential Medium (MEM) media containing 10% FBS to a uniform monolayer. Cells were then rinsed and transferred to bicarbonate-free MEM for 2 hours and then analyzed on the Seahorse Extracellular Flux (XF) Analyzer using the Mitochondria Stress Test Kit. The XF Analyzer measures the oxygen consumption rate (OCR) and the extracellular acidification rate (EACR; ref. 19) at intervals of approximately 2 to 5 minutes. OCR is an indicator of mitochondrial respiration, and ECAR is predominately the result of glycolysis.

Protein, RNA, and enzyme activity analyses

For Western blot analysis, protein samples were prepared in NuPAGE LDS sample buffer (Invitrogen) containing NuPAGE sample-reducing agent, boiled for 10 minutes, electrophoresed on a 4% to 12% Bis-Tris denaturing polyacrylamide gel (Invitrogen), and transferred to polyvinylidene difluoride membranes. Antibodies against the following proteins were used: GPx-1 and SBP1 (MBL, International), GAPDH and TRXRD (Proteintech) and MnSOD (BD Biosciences), GPx4 and β-actin (Abcam), and AKT, pAKT(Ser-473), and NF-κB p65 (Cell Signaling). Protein bands were quantified using ImageJ software (NIH) and normalized to β-actin band density.

High-performance liquid chromatography detection of superoxide using dihydroethidium

For detection of superoxide, cells were washed twice with Dulbecco's Phosphate Buffered Saline and incubated with Hank's Balanced Salt Solution containing 10 μmol/L dihydroethidium (DHE) for 60 minutes. Media were collected and centrifuged at 3,000 rpm for 5 minutes. Fluorescence analysis of the oxidation product 2-hydroxyethidium (EOH) was performed on a Beckman Coulter high-performance liquid chromatography (HPLC) system. Samples were separated on a Synergi-Fusion column (250 × 4.6 mm; Phenomenex) using a gradient elution of 10% v/v acetonitrile, 0.1% trifluoracetic acid solution as the mobile phase A and 100% acetonitrile as mobile phase B with a flow rate set at 1.00 mL/min. Runs began at 100% phase A. Phase B was increased linearly from 0% to 42% in 25 minutes, then reduced to 0% during 5 minutes, and kept at 0% for 5 minutes. The UV detector was set at 350 nm to monitor the elution of DHE. Fluorescence detection was measured using 480 nm (excitation) and 580 nm (emission). Authentic DHE and EOH standard solutions were injected onto the HPLC to determine the retention time of the corresponding peaks. All procedures were performed in the dark or under indirect light. Quantification was performed by normalizing the integrated peak areas with protein concentrations measured using the BCA Protein Reagent (Thermo Scientific).

Results

Allelic variants of GPx-1 differentially partition between the cytoplasm and the mitochondria

Most studies have focused on the investigation of the cytosolic activities of GPx-1 despite the demonstration that the enzyme also can reside within the mitochondria (20, 21). To assess the cellular location of the GPx-1 protein expressed by different alleles, cytoplasmic and mitochondrial cellular fractions were obtained from four previously generated MCF-7 transfectants containing either 5 or 7 alanine repeat codons (A5 or A7) and either a proline (P) or leucine (L) at codon 198, these being referred to as A5L, A7L, A5P, or A7P (9). The extracts were analyzed by Western blotting with anti–GPx-1 antibodies as well as with anti–COX-1 antibodies as a marker for mitochondrial protein expression. Consistent with several previous publications, GPx-1 was detected in both the cytoplasmic and mitochondrial fractions (20–23). However, this analysis indicated that there was a differential distribution between the cytoplasm and the mitochondria among the proteins encoded by the distinct GPx-1 alleles, with A7L being less distributed to the mitochondria as compared with A5P, A5L, and A7P (Fig. 1A and B). Pooling data by either the number of alanine repeats or the leucine/proline variation indicated that both genetic variations were contributing to determining cellular localization (Fig. 1C). These results were confirmed by assaying for GPx activity utilizing the same extracts as were used in the Western blotting shown in Figs. 1 and 2. Thus, quantification of protein levels and the measurement of GPx enzyme activity indicated a differential partitioning of GPx-1 between the cytoplasm and mitochondria, as well as the contribution of both the alanine repeats and the codon 198 polymorphism in determining that distribution.

MCF-7 cells expressing distinct GPx-1 alleles respond differently to oxidative stress

To investigate the consequences of allelic variation in the GPx-1 gene on reactive oxygen species (ROS) levels, we used roGFP directed to either the cytoplasm or mitochondria (cyto-RoGFP or mito-RoGFP, respectively). These constructs were delivered to cells by viral infection, and fluorescence was quantified by flow cytometry. Given the greatest differences among cells expressing distinct GPx-1 genotypes were between those expressing the A5P and A7L alleles, subsequent studies focused on just those two genotypes. The results of this analysis are shown in Fig. 3 and demonstrate that cells expressing the A7L allele, which partitioned to the greatest extent to the cytoplasm, also exhibited the lowest levels of oxidized GFP, both in the cytoplasm (Fig. 3A) and the mitochondria (Fig. 3B).

To assess whether there were differences in the response of MCF-7 cells expressing those GPx-1 alleles to oxidative stress, cells were exposed to 100 μmol/L *t*-BOOH and consequential changes in growth were assessed over 2 days (Fig. 4). Cells expressing A5P were more sensitive to *t*-BOOH than cells expressing A7L ($P < 0.05$).

Targeting GPx-1 exclusively to the mitochondria

All of the data presented above were conducted with naturally occurring GPx-1 alleles and indicated that the localization of GPx-1 proteins might have a significant impact on the cellular biology of the enzyme. To further investigate this possibility, a hybrid GPx-1 protein targeted to the mitochondria was generated by the fusion of the MnSOD MTS to the GPx-1 open reading frame. The constructs encoding the hybrid protein were transfected into MCF-7 cells. Transfectants that

Downloaded from http://aacrjournals.org/cancerres/article-pdf/74/18/5118/2708352/5118.pdf by guest on 15 February 2025

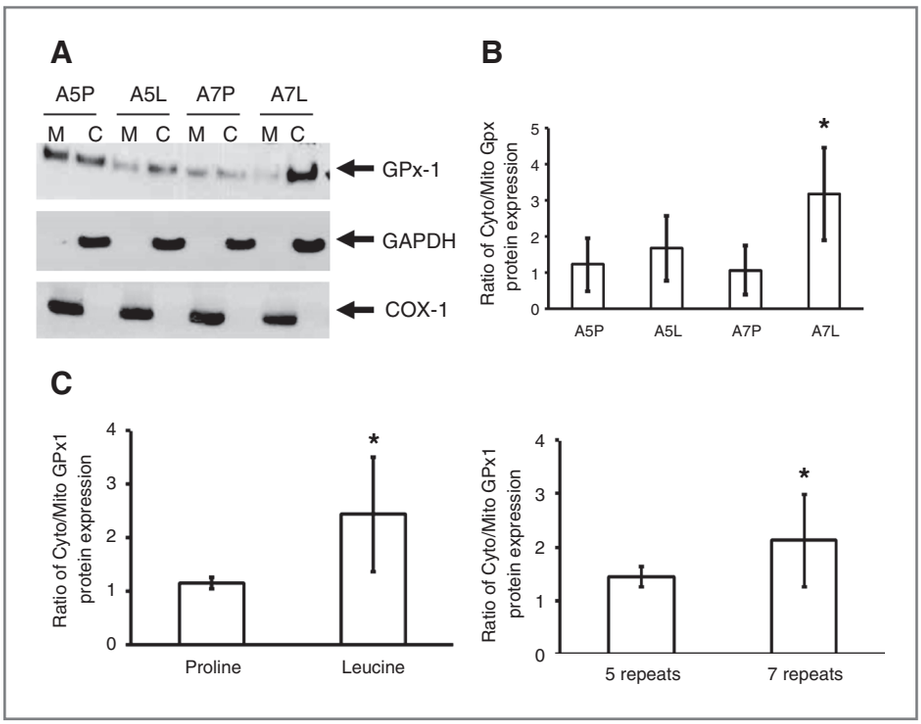

Figure 1. GPx-1 gene polymorphisms affect the cellular distribution between cytosolic and mitochondrial compartments. A, protein extracts were prepared from cells expressing different GPx-1 alleles and separated into cytoplasmic and mitochondrial fractions. Equal amounts of proteins were electrophoresed and visualized by Western blotting with anti–GPx-1 monoclonal antibodies as well as antibodies directed against GAPDH and COX-1 as indicators of cytoplasmic and mitochondrial proteins, respectively. B, densitometry was performed on independently prepared extracts and the ratio of the signals obtained from the cytoplasmic to the mitochondrial fractions was determined. C, the data were pooled by either the codon 198 polymorphism (proline vs. leucine) or by the number of alanine codons. *, $P < 0.005$ for A7L versus A5P in B, of 198P versus 198L in C, and 5 alanine repeats versus 7 repeats with $n = 6$.

expressed the mitochondrially targeted GPx-1 (mito-A5P and mito-A7L) were selected, which exhibited similar GPx enzyme activity levels (41.70 ± 1.1 units and 47.16 ± 1.9 units, respectively), similar to that achieved by the expression of the same two native, nontargeted A5P and A7L alleles (66.47 ± 5.4 units and 49.75 ± 4.5 units, respectively). As seen in Fig. 5A, examination of mitochondrial and cytoplasmic fractions from mito-A5P and mito-A7L expressing cells and examination by Western blotting indicated that the targeting was successful and these proteins partitioned exclusively to the mitochondria. Verification of successful targeting was achieved by confocal microscopy using GPx-1–specific antibodies and the Mitotracker Red dye to identify the location of the mitochondria (Fig. 5B).

Both GPx-1 cellular location and primary structure affect its biologic properties

The Seahorse XF24 XF analyzer permits the simultaneous determination of the ECAR (19), which is dominated by lactic acid generated as a result of glycolytic energy metabolism, and the OCR that is a measure of mitochondrial bioenergetic function (24). The relative use of mitochondrial respiration as compared with glycolysis can then be represented as the OCR/ECAR ratio (25). MCF-7 (GPx-1 null), MCF-7 cells expressing the A5P and A7L GPx-1 isoforms, and MCF-7 transfectants that express those same isoforms exclusively directed to the mitochondria were analyzed using the Seahorse platform (Fig. 6A). The baseline OCR/ECAR ratio was initially recorded, followed by the treatment of the cells with 1.5 μmol/L oligomycin to inhibit complex V of ATP synthase thus disrupting ATP production from the proton gradient. Cells were subsequently exposed to carbonylcyanide-4-(trifluoromethoxy)-phenylhydrazone to uncouple respiration, resulting in a measure of maximal respiratory rate, a sensitive measure of electron transport chain integrity and mitochondrial functional capacity. Finally, electron flow through complex I and III was blocked by treating the reaction with rotenone and antimycin A. The data presented in Fig. 6A surprisingly indicated that both cellular location and the primary amino acid sequence of the GPx-1 isoform affected energy metabolism in these cells, with the mitochondrially directed A7L isoform resulting in mitochondria significantly more active in electron transport as compared with cells expressing the other GPx-1 isoforms.

Next, we assessed the effects of GPx-1 cellular location on superoxide levels by measuring the oxidation of DHE by HPLC. Superoxide concentrations were 3- to 4-fold higher when cells expressed GPx-1 (Fig. 6B). However, this effect of GPx-1 was significantly diminished when that enzyme was restricted to the mitochondria.

Downloaded from http://aacrjournals.org/cancerres/article-pdf/74/18/5118/2708352/5118.pdf by guest on 15 February 2025

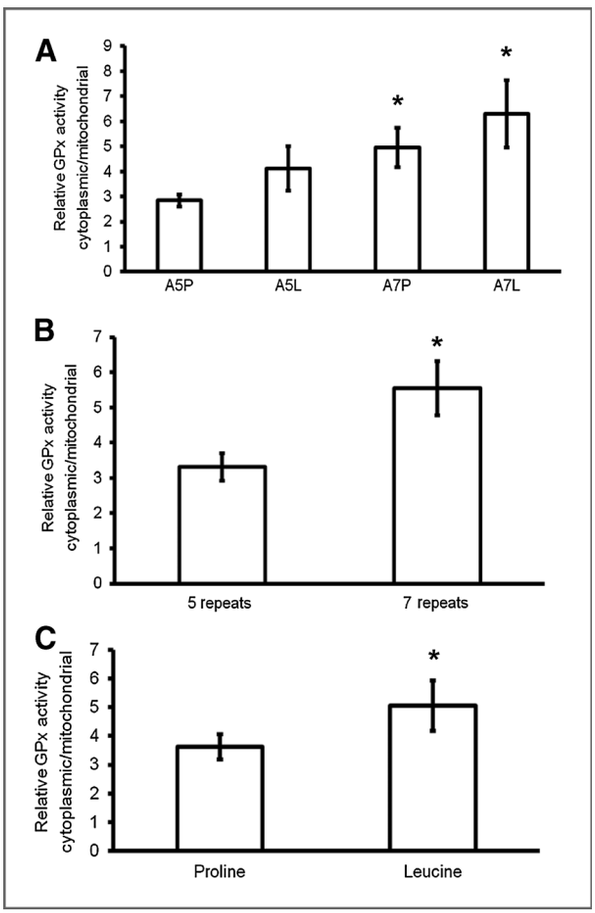

Figure 2. GPx activity in the cytoplasmic and mitochondrial fractions reflects the distribution pattern of the protein expressed from different GPx-1 alleles using the same extracts used to determine the levels of the GPx-1 protein in Fig. 1. A, enzyme activity was determined and the ratio of the activity obtained from the cytoplasmic to mitochondrial fractions is presented. The data were pooled by either the number of alanine codons (B) or the codon 198 polymorphism (proline vs. leucine; C). *, $P < 0.005$ for A7L and A7P versus A5P in A, the alanine repeats in B, or of 198P versus 198L in C, and the number of alanine repeats with $n = 6$.

As an additional means of assessing the impact of GPx-1 primary structure and cellular location, cells were treated with *t*-BOOH, and cell viability was determined after 48 hours by quantifying DNA with the blue-fluorescent Hoechst 33258 nucleic acid stain. As seen in Fig. 4, when A7L was directed to the mitochondria, the cells were less protected as compared with the MCF-7 cells expressing GPx-1 isoform in both the mitochondria and the cytoplasm (Fig. 4). The consequences of directing A5P to the mitochondria on resistance to *t*-BOOH were less clear given the reduced growth caused by the expression of mito-A5P.

Ectopic expression of GPx-1 isoforms has distinct effects on the expression of signaling proteins and other selenoproteins

It was investigated whether signaling molecules involved in cell growth and metabolism may be differentially affected by the GPx-1 proteins investigated here. Previously, we reported that enhanced GPx-1 expression could alter the phosphorylation of Akt (26), a protein kinase with multiple downstream targets that, when activated, can stimulate the switch from oxidative phosphorylation to glycolysis (reviewed in ref. 27). Increased levels of A5P, mito-A5P, A7L, or mito-A7L in MCF-7 cells did not change the levels of total Akt (Fig. 7). Increased expression of A5P dramatically reduced the levels of pAkt, whereas this was not seen with the mitochondrially targeted protein. In contrast, the expression of A7L increased the phosphorylation of Akt and did so slightly more when located exclusively to the mitochondria (Fig. 7).

GPx-1 downregulates NF-κB, a redox-sensitive transcription factor that affects cell survival, immunity, and other biologic processes (28, 29). As expected, overexpression of either A5P or A7L reduced the levels of the NF-κB, with this effect being stronger for A7L than A5P. Targeting of those isoforms to the mitochondria had opposing effects: mito-A5P reduced NF-κB more effectively than A5P, whereas mito-A7L only marginally reduced NF-κB levels.

Lastly, it was investigated whether the cellular location and allelic identity of GPx-1 had an effect on other selenium-containing proteins (Fig. 7). Although no effect was observed on the levels of thioredoxin reductase (TrxRD), a selenoprotein critical in maintaining the cellular redox environment, the levels of GPx-4, a membrane-associated member of the GPx family, were affected by both GPx-1 genotype and location. Expression of A5P dramatically reduced the levels of GPx-4 while targeting A5P to the mitochondria also reduced GPx-4 levels, but to a lesser extent. The expression of A7L also reduced the levels of GPx-4 but not to the extent seen with A5P, but in contrast to that seen with A5P, mito-A7L was more effective in reducing GPx-4 levels (Fig. 7). Selenium binding protein-1 (SBP1) is a non-selenocysteine containing selenoprotein whose levels are inversely associated with GPx-1 activity and is typically expressed at lower levels in tumors compared with the corresponding normal tissue (30). Expression of either A5P or A7L reduced the levels of SBP1 in MCF-7 cells, although this effect was considerably less when GPx-1 was targeted to the mitochondria (Fig. 7).

Discussion

These studies were initiated to elucidate the biologic consequences of GPx-1 allelic variations and to begin to establish a role for these variations in cancer risk. A role for GPx-1 in determining cancer risk might not be unexpected as a primary function of GPx-1 is to reduce levels of H_2O_2. Although more stable and less reactive than other ROS, H_2O_2 might contribute to the direct oxidation of proteins and nucleic acids, or H_2O_2 can be converted into much more reactive ROS, such as the hydroxyl radical by redox active metals. In addition to direct oxidative damage to biomolecules, aerobic organisms have also evolved to use ROS as potent signaling molecules. Fluctuations in the levels and types of ROS can be due to changes in the cellular microenvironment or intrinsic metabolic adaptations, and examples abound throughout phylogeny, indicating the sensing and response to H_2O_2. A significant component of ROS signaling is the consequence of the oxidation of reactive

Downloaded from http://aacrjournals.org/cancerres/article-pdf/74/18/5118/2708352/5118.pdf by guest on 15 February 2025

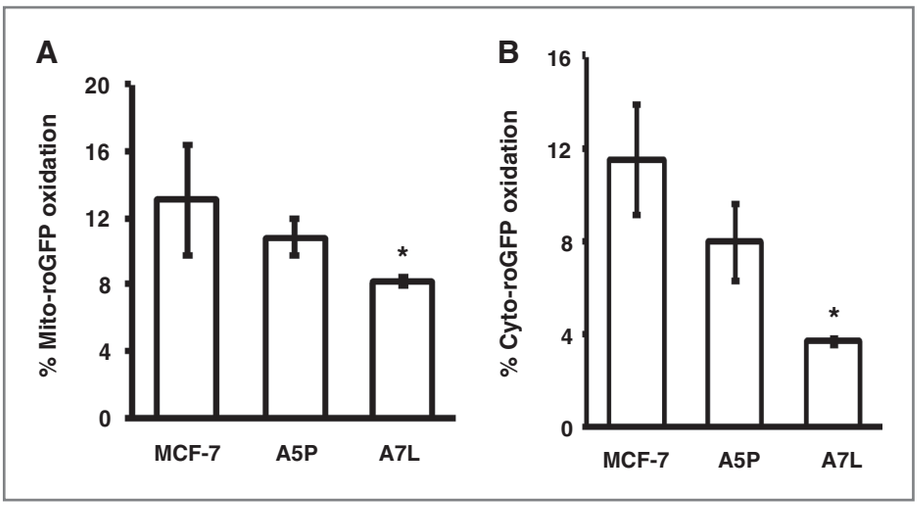

Figure 3. GPx-1 allelic identity affects ROS generation. MCF-7 cells either transfected with vector or either A5P or A7L were used to assess mitochondrial and cytoplasmic ROS levels using mito-roGFP (A) and cyto-roGFP (B). ro-GFP oxidation was determined by flow cytometry as described in Materials and Methods. *, $P < 0.05$ versus MCF vector control with $n = 6$.

cysteine residues in catalytic proteins and one estimate postulates that over 500 individual proteins might be regulated in this manner, with many being tyrosine and multi-specific phosphatases (31, 32).

A principal result reported in this article was that the selected GPx-1 allelic variants distributed differently between the mitochondria and cytoplasm. The lack of detectable GPx-1 levels in MCF-7 cells made it possible to examine the consequences of the sequence variations in the same cellular environment by ectopically expressing these proteins from expression constructs, thus minimizing the potential contributions of other proteins or factors that might differ across individual cell lines. How GPx-1 partitions to mitochondria remains unknown, particularly as its primary sequence lacks a canonical MTS. The surprising observation that the A7L allele distributed differently than the other variants examined (A5P, A5L, and A7P) indicates that there is an interaction between those variable amino acids located at opposite ends of the protein, perhaps by affecting GPx-1 higher-order structure and/or its interaction with other proteins that affect its mitochondrial transport. To date, there is limited information about GPx-1 binding proteins. However, physical interaction with the Abl/Arg tyrosine kinase (33) and selenium binding protein 1, or SBP1 (34), has been reported. The interaction between the alanine repeat motif and the polymorphism at codon 198 may explain the lack of consistency observed among independent epidemiologic studies examining the effect of these variations on cancer risk. To date, there are currently no reports examining associations among cancer risk and both variations in the same population.

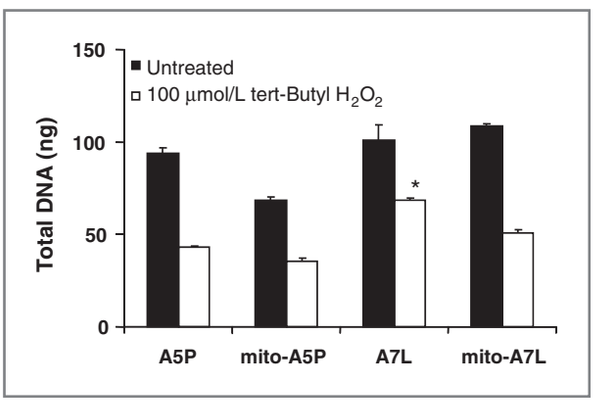

Figure 4. GPx-1 allelic identity affects viability after challenge with ROS. Cells expressing either A5P, A7L, mitochondria-targeted A5P (mito-A5P), or mitochondria-targeted A7L (mito-A7L) were challenged with 100 μmol/L *t*-BOOH for 48 hours and viability determined. The difference between A5P and A7L following exposure to *t*-BOOH was significant at *, $P < 0.05$. Error bars, SD with $n = 6$.

The generation of a derivative GPx-1 protein that exclusively partitions to the mitochondria provided direct evidence that the cellular localization of that protein can have a profound effect on cell biology, including resistance to oxidative stress, energy metabolism, and signaling. As such, these results provide new evidence for the functionality of these variations and support the existing epidemiologic data linking them to disease risk. How the localization of GPx-1 affects these endpoints remains to be determined. GPx-1–specific enzyme activity may be higher in the mitochondria than the cytoplasm due to its availability for posttranslational activation. Recently, two studies have indicated that chronic alcohol consumption and ablation of SIRT3, a mitochondrial deacetylase, leads to hyper-acetylation of several proteins, including GPx-1 (35, 36). Acetylation of GPx-1 was also noted in a recent proteomic analysis that mapped lysine acetylation sites of various proteins across rat tissues and identified 5 potential acetylated lysines in the antioxidant protein (37). It is noteworthy that the GPx-1 allele encoding a leucine at codon 198 is most often associated with elevated disease risk (7, 38) and may be localized preferentially to the cytoplasm where it would be unavailable for deacetylation and presumed activation by Sirt3. GPx-1 levels and specific activity in the mitochondria may (i) affect the susceptibility of proteins to oxidative damage, (ii) influence signaling mediated by the efflux of H_2O_2

Downloaded from http://aacrjournals.org/cancerres/article-pdf/74/18/5118/2708352/5118.pdf by guest on 15 February 2025

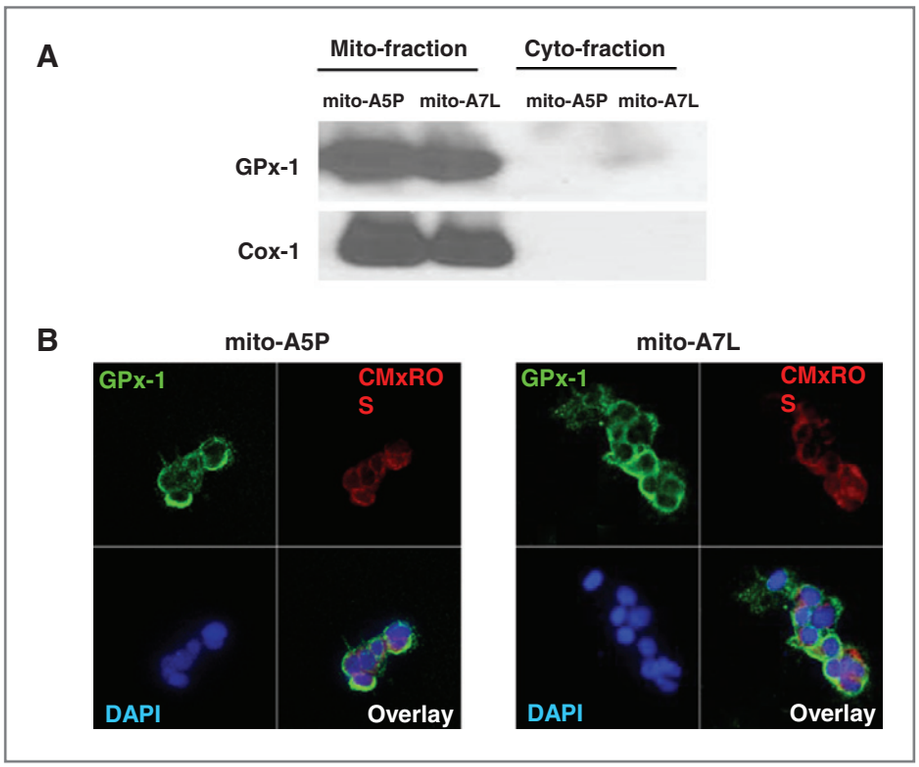

Figure 5. Molecular targeting of the A5P and A7L GPx-1 to the mitochondria. Constructs engineered to express the A5P or A7L GPx-1 alleles were targeted to the mitochondria by attaching the MTS sequence encoded by the mitochondrial MnSOD gene, and these constructs were transfected into GPx-1 null MCF-7 cells, selected in antibiotic, and expanded for analysis. A, protein extracts were prepared, separated into mitochondrial and cytoplasmic fractions, and analyzed by Western blotting with anti–GPx-1 antibodies. B, the localization of mitochondrially directed GPx-1 was confirmed in individual transfectants by immunohistochemistry and subsequent confocal imaging, where GPx-1 is seen to be exclusively colocalized with mitotracker (red fluorescence) in the transfectants. Nuclei were stained with DAP1 (blue fluorescence).

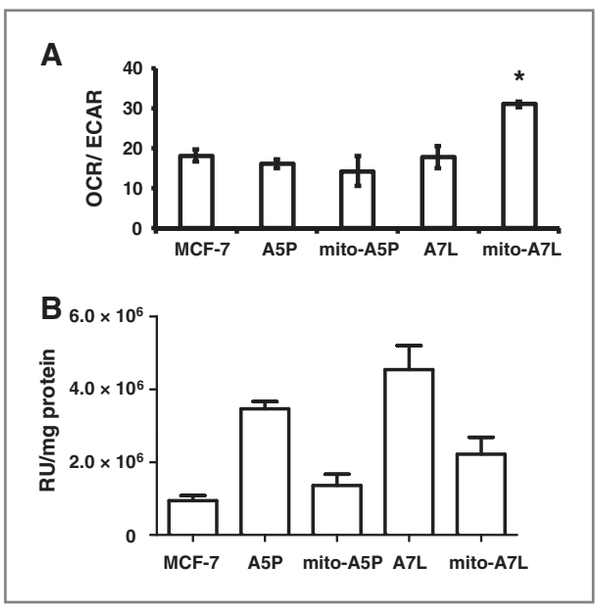

Figure 6. GPx-1 allelic identity and cellular localization affect mitochondrial metabolism. A, OCRs were determined in cells expressing either GPx-1 variants or vector using the Sea Horse XF analyzer platform. Data were calculated using the XF Wave software supplied with the analyzer. *, $P < 0.005$; from MCF7 with $n = 3$. B, the levels of superoxide in MCF-7 transfectants expressing A5P, A7L, mito-A5P, or mito-A7L were determined by measuring the oxidation of DHE. The differences between A5P and mito-A5P, and between A7L and mito-A5L were significant at $P < 0.05$ with $n = 3$.

generated by the dismutation of superoxide by the mitochondrially located MnSOD protein, or (iii) affect the availability of H_2O_2 to serve as a substrate for the recently discovered peroxidase activity of MnSOD (39), resulting in mitochondrial damage, and predisposing to cancer.

The complexity of the data obtained by comparing the effects of the different GPx-1 isozymes on both biologic and molecular endpoints indicates that both the primary sequence and cellular location affect signaling pathways that may account for the associations between GPx-1 genotype and cancer. The expression of distinct GPx-1 alleles resulted in differences in ROS species that were noted by using roGFP as an indicator of ROS, both in the cytoplasm and in the mitochondria, and differences in superoxide levels were observed using DHE detection. The particular species of ROS and their compartmentalization are likely to contribute to the divergent patterns of activation of signaling pathways, such as those affected by Akt and NF-κB activity seen when different GPx-1 alleles were expressed. GPx-1 has been shown to reduce the transcription of SBP1 as well as to physically interact with that protein (30, 34). It is therefore plausible that the sequestration of GPx-1 in the mitochondria makes it less available to interact with SBP1, a predominantly cytoplasmic protein, or makes it less efficient at reducing H_2O_2 that can stimulate SBP1 transcription via a ROS-responsive antioxidant response element located 5′ to the SBP1 promoter. Collectively, these data provide novel insight into the consequences of GPx-1 genotype and provide plausible mechanisms by which different GPx-1 alleles can contribute to cancer risk.

Downloaded from http://aacrjournals.org/cancerres/article-pdf/74/18/5118/2708352/5118.pdf by guest on 15 February 2025

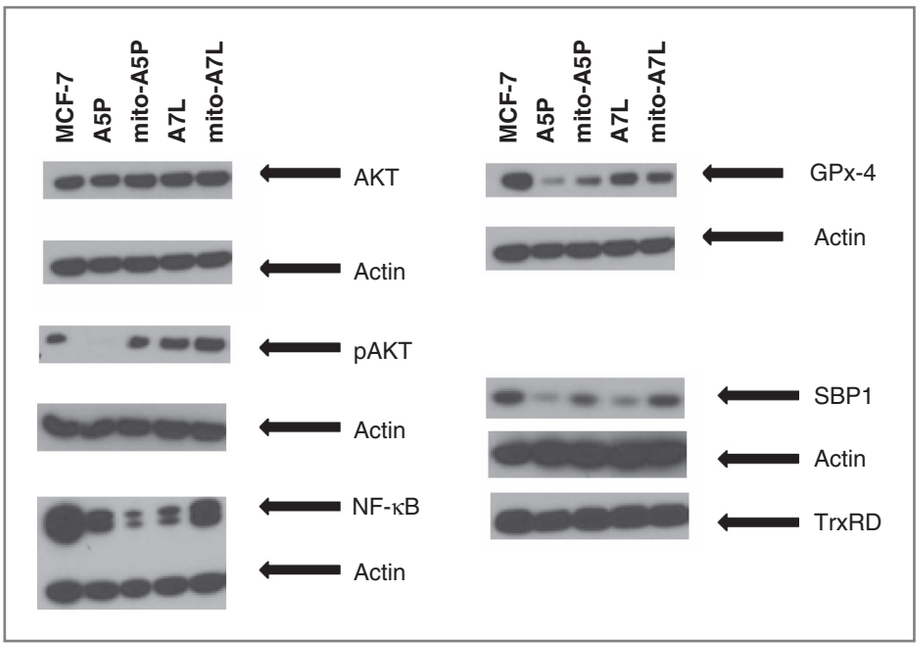

Figure 7. Expression of GPx-1 isozymes affects the levels of signaling and selenium-containing proteins. Protein extracts were prepared from the indicated cells and analyzed using protein-specific antibodies. Actin levels were determined as an indication of equal loading of protein on the gel.

Disclosure of Potential Conflicts of Interest

No potential conflicts of interest were disclosed.

Authors' Contributions

Conception and design: S. Bera, F. Weinberg, M.G. Bonini, A.M. Diamond
Development of methodology: S. Bera, F. Weinberg, M.G. Bonini
Acquisition of data (provided animals, acquired and managed patients, provided facilities, etc.): S. Bera, F. Weinberg, D.N. Ekoue, K. Ansenberger-Fricano, M. Mao, M.G. Bonini
Analysis and interpretation of data (e.g., statistical analysis, biostatistics, computational analysis): S. Bera, F. Weinberg, D.N. Ekoue, K. Ansenberger-Fricano, M. Mao, M.G. Bonini
Writing, review, and/or revision of the manuscript: S. Bera, F. Weinberg, D.N. Ekoue, K. Ansenberger-Fricano, M. Mao, A.M. Diamond
Administrative, technical, or material support (i.e., reporting or organizing data, constructing databases): S. Bera
Study supervision: A.M. Diamond

Grant Support

This work was supported by a grant from the NIH (grant RO1CA127943; A.M. Diamond), a Post Doctoral Fellowship from the American Institute for Cancer Research (grant 10A072; S. Bera), and by a grant from the Department of Defense (W911NF-07-R-0003-04; M.G. Bonini).

The costs of publication of this article were defrayed in part by the payment of page charges. This article must therefore be hereby marked *advertisement* in accordance with 18 U.S.C. Section 1734 solely to indicate this fact.

Received March 4, 2014; revised June 20, 2014; accepted July 7, 2014; published OnlineFirst July 21, 2014.

References

1. Lubos E, Loscalzo J, Handy DE. Glutathione peroxidase-1 in health and disease: from molecular mechanisms to therapeutic opportunities. Antiox Redox Signal 2011;15:1957–97.
2. Berry MJ, Banu L, Chen Y, Mandel SJ, Kiefer JD, Harney JW, et al. Recognition of UGA as a selenocysteine codon in Type I deiodinase requires sequences in the 3′ untranslated region. Nature 1991;353:273–6.
3. Caban K, Copeland PR. Size matters: a view of selenocysteine incorporation from the ribosome. Cell Mol Life Sci 2006;63:73–81.
4. Driscoll DM, Copeland PR. Mechanism and regulation of selenoprotein synthesis. Annu Rev Nutr 2003;23:17–40.
5. Hatfield DL, Gladyshev VN. How selenium has altered our understanding of the genetic code. Mol Cell Biol 2002;22:3565–76.
6. Rayman MP. Selenoproteins and human health: insights from epidemiological data. Biochim Biophys Acta 2009;1790:1533–40.
7. Zhuo P, Diamond AM. Molecular mechanisms by which selenoproteins affect cancer risk and progression. Biochim Biophys Acta 2009;115:227–42.
8. Hu YJ, Diamond AM. Role of glutathione peroxidase 1 in breast cancer: loss of heterozygosity and allelic differences in the response to selenium. Cancer Res 2003;63:3347–51.
9. Zhuo P, Goldberg M, Herman L, Lee BS, Wang H, Brown RL, et al. Molecular consequences of genetic variations in the glutathione peroxidase 1 selenoenzyme. Cancer Res 2009;69:8183–90.
10. Cox DG, Hankinson SE, Kraft P, Hunter DJ. No association between GPX1 Pro198Leu and breast cancer risk. Cancer Epidemiol Biomarkers Prev 2004;13:1821–2.
11. Knight JA, Onay UV, Wells S, Li H, Shi EJ, Andrulis IL, et al. Genetic variants of GPX1 and SOD2 and breast cancer risk at the Ontario site of the Breast Cancer Family Registry. Cancer Epidemiol Biomarkers Prev 2004;13:146–9.
12. Winter JP, Gong Y, Grant PJ, Wild CP. Glutathione peroxidase 1 genotype is associated with an increased risk of coronary artery disease. Coron Artery Dis 2003;14:149–53.
13. Miller AD, Rosman GJ. Improved retroviral vectors for gene transfer and expression. Biotechniques 1989;7:980–90.
14. Magalhaes PJ, Andreu AL, Schon EA. Evidence for the presence of 5S rRNA in mammalian mitochondria. Mol Biol Cell 1998;9:2375–82.
15. Samuels BA, Murray JL, Cohen MB, Safa AR, Sinha BK, Townsend AJ, et al. Increased glutathione peroxidase activity in human sarcoma cell line with inherent doxorubicin resistance. Cancer Res 1991;51:521–7.
16. Handy DE, Hang G, Scolaro J, Metes N, Razaq N, Yang Y, et al. Aminoglycosides decrease glutathione peroxidase-1 activity by interfering with selenocysteine incorporation. J Biol Chem 2006;281:3382–8.
17. Tobe R, Naranjo-Suarez S, Everley RA, Carlson BA, Turanov AA, Tsuji PA, et al. High error rates in selenocysteine insertion in mammalian

Downloaded from http://aacrjournals.org/cancerres/article-pdf/74/18/5118/2708352/5118.pdf by guest on 15 February 2025

cells treated with the antibiotic doxycycline, chloramphenicol, or geneticin. J Biol Chem 2013;288:14709–15.
18. Dooley CT, Dore TM, Hanson GT, Jackson WC, Remington SJ, Tsien RY. Imaging dynamic redox changes in mammalian cells with green fluorescent protein indicators. J Biol Chem 2004;279:22284–93.
19. Eggler AL, Gay KA, Mesecar AD. Molecular mechanisms of natural products in chemoprevention: induction of cytoprotective enzymes by Nrf2. Mol Nutr Food Res 2008;52 Suppl 1:S84–94.
20. Flohe L, Schlegel W. [Glutathione peroxidase. IV. Intracellular distribution of the glutathione peroxidase system in the rat liver]. Hoppe Seylers Z Physiol Chem 1971;352:1401–10.
21. Utsunomiya H, Komatsu N, Yoshimura S, Tsutsumi Y, Watanabe K. Exact ultrastructural localization of glutathione peroxidase in normal rat hepatocytes: advantages of microwave fixation. J Histochem Cytochem 1991;39:1167–74.
22. Esworthy RS, Ho YS, Chu FF. The Gpx1 gene encodes mitochondrial glutathione peroxidase in the mouse liver. Arch Biochem Biophys 1997;340:59–63.
23. Sies H, Moss KM. A role of mitochondrial glutathione peroxidase in modulating mitochondrial oxidations in liver. Eur J Biochem 1978;84: 377–83.
24. Wu M, Neilson A, Swift AL, Moran R, Tamagnine J, Parslow D, et al. Multiparameter metabolic analysis reveals a close link between attenuated mitochondrial bioenergetic function and enhanced glycolysis dependency in human tumor cells. Am J Physiol Cell Physiol 2007;292: C125–36.
25. Gohil VM, Sheth SA, Nilsson R, Wojtovich AP, Lee JH, Perocchi F, et al. Nutrient-sensitized screening for drugs that shift energy metabolism from mitochondrial respiration to glycolysis. Nat Biotechnol 2010;28:249–55.
26. Nasr M, Fedele MJ, Esser KA, Diamond AM. GPX-1 modulates AKT and $P70^{S6K}$ phosphorylation and GADD45 levels in MCF-7 cells. Free Rad Biol Med 2004;37:187–95.
27. Plas DR, Thompson CB. Akt-dependent transformation: there is more to growth than just surviving. Oncogene 2005;24:7435–42.
28. Kretz-Remy C, Mehlen P, Mirault ME, Arrigo AP. Inhibition of I kappa B-alpha phosphorylation and degradation and subsequent NF-kappa B activation by glutathione peroxidase overexpression. J Cell Biol 1996;133:1083–93.
29. Li Q, Sanlioglu S, Li S, Ritchie T, Oberley L, Engelhardt JF. GPx-1 gene delivery modulates NFkappaB activation following diverse environmental injuries through a specific subunit of the IKK complex. Antiox Redox Signal 2001;3:415–32.
30. Ansong E, Yang W, Diamond AM. Molecular cross-talk between members of distinct families of selenium containing proteins. Mol Nutr Food Res 2014;58:117–23.
31. Weerapana E, Wang C, Simon GM, Richter F, Khare S, Dillon MB, et al. Quantitative reactivity profiling predicts functional cysteines in proteomes. Nature 2010;468:790–5.
32. Finkel T. Signal transduction by reactive oxygen species. J Cell Biol 2011;194:7–15.
33. Cao C, Leng Y, Huang W, Liu X, Kufe D. Glutathione peroxidase 1 is regulated by the c-Abl and Arg tyrosine kinases. J Biol Chem 2003;278:39609–14.
34. Fang W, Goldberg ML, Pohl NM, Bi X, Tong C, Xiong B, et al. Functional and physical interaction between the selenium-binding protein 1 (SBP1) and the glutathione peroxidase 1 selenoprotein. Carcinogen 2010;31:1360–6.
35. Shepard BD, Tuma DJ, Tuma PL. Chronic ethanol consumption induces global hepatic protein hyperacetylation. Alcohol Clin Exp Res 2010;34:280–91.
36. Fritz KS, Galligan JJ, Hirschey MD, Verdin E, Petersen DR. Mitochondrial acetylome analysis in a mouse model of alcohol-induced liver injury utilizing SIRT3 knockout mice. J Proteome Res 2012;11: 1633–43.
37. Lundby A, Lage K, Weinert BT, Bekker-Jensen DB, Secher A, Skovgaard T, et al. Proteomic analysis of lysine acetylation sites in rat tissues reveals organ specificity and subcellular patterns. Cell Rep 2012;2:419–31.
38. Rayman MP. Selenium and human health. Lancet 2012;379: 1256–68.
39. Ansenberger-Fricano K, Ganini D, Mao M, Chatterjee S, Dallas S, Mason RP, et al. The peroxidase activity of mitochondrial superoxide dismutase. Free Rad Biol Med 2013;54:116–24.

Downloaded from http://aacrjournals.org/cancerres/article-pdf/74/18/5118/2708352/5118.pdf by guest on 15 February 2025